Relational Cosmological Superposition Theory: From the Informational Metric to Cosmology

Extensión del programa AQUAL relacional con estructura causal, transiciones $R \leftrightarrow S$, límites luminosos y contornos cosmológicos atemporales

Autor(es)
Javier Martínez Torregrosa
Investigador independiente

September 9, 2025

Abstract

We propose a complete relational theory in which *physical variables are not primitive* but rather *emergent* from patterns of correlation. We postulate two ontological regimes: a S *silent* state, of zero relational entropy, *timeless* and *ageometric*, and a set of R *relational* states, where the growth of relational entropy S_R enables a notion of time and an effective metric. The observer/observed separation is modeled as a *choice of factorization* of the Hilbert space, and it is precisely that choice which *makes variables like space, time, and gravity exist*.

Formally, we define S_R as a sum of mutual information terms over families of bipartitions and reconstruct a metric $g_{\mu\nu}[I]$ from diffusion distances in the correlation graph. We show that *informational null trajectories* (those with minimal variation $\delta S_R = 0$) define the causal boundary and provide an *informational interpretation* of c; coherent electromagnetic modes approximate this limit and act as *windows* from the R domain to S. The effective dynamics is implemented by means of an AQUAL-type action with an environmental acceleration scale $a_0(S)$; we demonstrate stability (absence of ghosts) in the 4D scalar–tensor extension and guarantee Lorentzian signature in the metric reconstruction.

At cosmic scale, we replace initial/final conditions with *atemporal boundaries* in S and derive Friedmann-type effective equations with $a_0(S)(z)$. Two paths lead $R \to S$: *extreme dispersion* (homogenization of correlations) and *extreme concentration* (operatively dimensionless curvature). We present quantitative predictions and falsifiers: RAR band and evolution, strong lenses with the *same* μ and $a_0(S)$, photon coherence versus $\|\nabla S\|$, BTFR shifts, speed/non-dispersion of gravitational waves, and a CMB/BAO/$f\sigma_8$ fitting scheme to compare with ΛCDM. The theory thus becomes *operational and falsifiable* from the galactic scale to the cosmological scale.

Abstract

Planteamos una teoría relacional completa en la que *las variables físicas no son primitivas* sino *emergentes* desde patrones de correlación. Postulamos dos regímenes ontológicos: un estado S *silente*, de entropía relacional nula, *atemporal* y *ageométrico*, y un conjunto de estados R *relacionales*, donde el crecimiento de la entropía relacional S_R habilita una noción de tiempo y una métrica efectiva. La separación observador/observado se modela como una *elección de factoración* de la hilbertiana, y es precisamente esa elección la que hace *existir* variables como espacio, tiempo y gravedad.

Formalmente, definimos S_R como una suma de informaciones mutuas sobre familias de biparticiones y reconstruimos una métrica $g_{\mu\nu}[I]$ a partir de distancias de difusión en el grafo de correlaciones. Mostramos que las *trayectorias nulas informacionales* (aquellas con variación mínima $\delta S_R = 0$) definen el borde causal y proporcionan una *lectura informacional* de c; los modos electromagnéticos coherentes aproximan este límite y actúan como *ventanas* del dominio R hacia S. La dinámica efectiva se implementa mediante una acción tipo

AQUAL con una escala de aceleración ambiental $a_0(S)$; demostramos estabilidad (ausencia de fantasmas) en la extensión 4D escalar–tensor y garantizamos firma Lorentziana en la reconstrucción métrica.

A escala cósmica, reemplazamos condiciones inicial/final por *contornos atemporales* en S y derivamos ecuaciones efectivas tipo Friedmann con $a_0(S)(z)$. Dos rutas llevan $R \to S$: *dispersión extrema* (homogeneización de correlaciones) y *concentración extrema* (curvatura operativamente adimensional). Presentamos predicciones cuantitativas y falsadores: banda y evolución de la RAR, lentes fuertes con la *misma* μ y $a_0(S)$, coherencia fotónica frente a $\|\nabla S\|$, desplazamientos BTFR, velocidad/no-dispersión de ondas gravitacionales y un esquema de ajuste CMB/BAO/$f\sigma_8$ para comparar con ΛCDM. La teoría resulta así *operacional y falsable* desde la escala galáctica a la cosmológica.

Contents

1 Introduction

The starting premise is *relational and strong*: the universe does not *have* space, time, and gravity as prior ingredients; rather, it *comes* to have them when certain relationships between groupings of energy states stabilize. We will call R the regime where those relationships proliferate and can be quantified by a relational entropy S_R; then a *temporal order* appears and a *metric* that measures nearness in the fabric of correlations. In contrast, in the S regime — *silent* —, $S_R \to 0$: there is no before or after, nor trajectories or distances with operational meaning. In S, excitations can exist *without geometric support*, such as highly coherent electromagnetic modes,

but they lack geometric meaning until dynamics *places* them in an R context where there are observers, observed, and stable partitions of the degrees of freedom.

This relational vision ties in with classical ideas such as Mach's principle and modern proposals of the absence of absolute time (for example, Barbour's developments on a timeless universe emerging from configurations[1]). However, our approach goes further by quantitatively formulating said emergence through correlation entropy: space-time and gravity *appear* when the relational information S_R grows, aligned with the intuition that it is the physical relationships (and not a preexisting background) that define the geometry and the dynamics.

Observer/observed cut and emergence of variables. The distinction between observer and observed is not a linguistic accident: we formalize it as a *choice of factorization* $\{\mathcal{H} = \bigotimes_i \mathcal{H}_i\}$ for which the mutual information I_{ij} is robust under *coarse-graining*. Only under *R–admissible* factorizations does it make sense to talk about *variables* — positions, durations, forces — and *effective laws*. Strictly speaking, *variables appear when there is someone who can distinguish them*; and that distinction is, physically, stable correlation. For example, analogously to quantum decoherence, a physical system acquires defined properties only when it interacts stably with an environment or "observer" that records those properties. In our context, the choice of an R–admissible factorization (an observer/observed cut) plays that role: it defines which degrees of freedom act as "measuring apparatus" and which as "system", causing variables like position or energy to have operational meaning only after stable correlations are established between them.

Time as relational order. We define S_R as the sum of mutual informations over a family of bipartitions. The hypothesis — empirically fruitful — is that S_R *typically grows* and therefore induces a parameter $T = T(S_R)$ that we call *emergent time*. The "passage of time" is thus not an external flow, but the macroscopic shadow of the increase of useful correlation in the factorization that defines our R world.

From correlations to geometry. To quantify relational proximities, we construct a correlation graph with weights $W_{ij} = h(I_{ij})$, a Laplacian L, and a diffusion kernel $K_t = \exp[-tf(L)]$; the diffusion distance $d_t(i,j) = \|K_t(i,\cdot) - K_t(j,\cdot)\|_2^2$ induces an *effective spatial metric* at scale t. This recipe captures a simple intuition: strongly correlated systems appear "close"; decoupled systems, "far".

Causal structure and informational meaning of c. We elevate spatial geometry to a space–time structure by postulating that *informational null trajectories* are those along which the relational variation *does not increase*: $\delta S_R = 0$. This axiom fixes the *light cone* of the emergent metric and gives a natural reading of the *luminal bound* c: it is the propagation limit for signals that do not need to "spend" additional relational entropy. Coherent photons — nearly informationally null — thus play the role of *windows* from R to S: they trace the boundary where the geometric description touches its own foundation.

Effective dynamics and role of the environment. In the quasistatic (galactic) regime we use an AQUAL-type scalar action with a monotonic interpolating function $\mu(x)$ and an *environmental acceleration scale* $a_0(S)$ that encapsulates how the relational environment modulates the gravitational response. This choice satisfies three requirements: (i) *non-circularity* (the S field is constructed without resorting to V or g), (ii) correct *Newtonian limit*, and (iii) *monotonicity* (no ad hoc tricks in μ). We show how a *fundamental* functional $S[\rho]$ — defined on correlations — projects, under assumptions of quasistaticity and symmetry, into the operational construction $S = K_\sigma * \Sigma_b$, so that "ambient S" is a *coarse-graining* of "fundamental S".

4D extension and stability. To articulate the theory at large scale, we introduce a 4D scalar–tensor action with an informational term and $\Psi = \Phi$ (which ensures $\gamma_{\rm PPN} = 1$). We prove conditions of *linear stability* (positivity of the kinetic and gradient terms, *no ghosts* nor ultrasonic instability) and show how the quasistatic limit recovers the AQUAL equation. Furthermore, we show that the reconstruction $g_{\mu\nu}[I]$ obtains *Lorentzian signature* without ambiguities, such that the null cones defined by $\delta S_R = 0$ coincide with those of the effective metric.

Relational cosmology and boundaries in S. At homogeneous and isotropic scales, we integrate the informational component into Friedmann-type effective equations with $a_0(S)(z)$ and propose *atemporal boundaries in S* instead of initial/final conditions: the "before" and "after" of any Big Bang are *internal* descriptions within the R domain. This framework allows us to confront *directly* with CMB, BAO and $f\sigma_8$, and compare against ΛCDM without introducing *ad hoc* parameters.

Two return routes $R \to S$. The relational regime can collapse in two extreme ways: (i) via *dispersion* — when homogenization erases correlational contrasts and the geometric language loses meaning —, or (ii) via *concentration* — when the effective curvature grows until space becomes *operatively dimensionless*, idealizing the black hole scenario. In both cases, the result is the same: a return to S.

The rest of the manuscript develops these points with formal detail and with an operational emphasis: every philosophical idea is anchored in a mathematical definition, and every definition is connected to an empirical test or a falsifiable inequality.

2 Extended relational axioms and factorizations

In this section, we formalize the postulates of the relational framework, making explicit the S/R regimes, the role of factorizations of the Hilbert space in the emergence of physical variables, and the operational definition of the relational entropy S_R. We also introduce quantifiable criteria for $R \to S$ phase transitions and a measure on the space of relational configurations. An *operational summary* of axioms and hypotheses used in Secs. 2–3 is compiled in **Table 1**.

Axiom 1 (Ontological regimes S and R). *There exist two complementary ontological regimes: (i) a silent state S, characterized by zero relational entropy ($S_R = 0$), timeless and ageometric; and (ii) a set of relational states R with $S_R > 0$, in which the increase of S_R enables an arrow of time and an effective metric between degrees of freedom.*
Justification.— The S sector represents a "relational vacuum" without correlations; in R, patterns of correlation proliferate that make notions of distance, duration, and causality operative. The framework fits with the relational thesis already outlined in the Introduction (see the motivation and the observer/observed cut on pp. 2–3 of the manuscript; *see also* **Table 1**).

Axiom 2 (Factorization and role of the observer). *The observer/system distinction is modeled by a choice of factorization of the global Hilbert space $\mathcal{H} = \bigotimes_i \mathcal{H}_i$. Physical variables emerge from patterns of correlation (entanglement) between the subspaces induced by that factorization.*
Justification.— Under R–admissible factorizations (defined below), the mutual information between subfactors stabilizes operational variables (positions, effective times, potentials), in line with the approach already stated in the Introduction (*see* **Table 1**, A2).

Definition 1 (Relational entropy and R–admissible partitions). Let ρ be a state in $\mathcal{H}$ and $\mathcal{P} = \{(A, B)\}$ a family of bipartitions. We define

$$S_R[\rho; \mathcal{P}] \;=\; \sum_{(A,B)\in\mathcal{P}} I(A{:}B), \qquad I(A{:}B) \;=\; S(\rho_A) + S(\rho_B) - S(\rho_{AB})\;, \tag{1}$$

where $S(\cdot)$ is the von Neumann entropy. We will say that $\mathcal{P}$ is *R–admissible* if it satisfies: (i) *robustness under coarse–graining* (the value of S_R varies only marginally under finite groupings/refinements of subdegrees of freedom), and (ii) *coherent metricity*: the induced correlation graph (weights $W_{ij} \propto \mathcal{I}_{ij}$) is connected and its diffusive distance yields a well-defined spatial metric (Sec. 3).

Proposition 1 (Relational time arrow). *In generic physical evolutions under macroscopic constraints, S_R typically does not decrease; therefore $T = T(S_R)$ defines a temporal order. In the limit $S_R \to 0$ (S sector), geometric variables lack meaning.*
Sketch.— The statistical increase of useful correlations (mutual information) under local interactions makes S_R on average non-decreasing; negative fluctuations require fine tuning and are negligible at macroscopic scale.

2.1 R to S phase transitions: dispersion and concentration

Fixing small thresholds $\varepsilon, \delta > 0$, we define: *R phase*: $S_R \geq \varepsilon$ (with $|\dot{S}_R| \not< \delta$ typically); *S phase*: $S_R < \varepsilon$ and/or $|\dot{S}_R| < \delta$. We identify two extreme routes toward $R \to S$:

Route A (extreme dispersion). Correlational homogenization: $S_R \to S_R^{\max}$ with $\|\nabla S_R\| \to 0$ broadly. Operationally, contrasts disappear and the metric is lost (every region "looks like" any other).

Route B (extreme concentration). Concentration of correlations and increasing effective curvature until space becomes *operatively dimensionless*. Practical criterion: an informational curvature invariant (e.g. the inverse of the curvature radius extracted from diffusive distances) diverges, so that the curvature length L_c tends to zero and the notion of separation collapses. Both routes cause loss of time arrow ($\dot{S}_R \to 0$) and return the system to the silent sector S (*see the diagram* in **Fig. 1**).

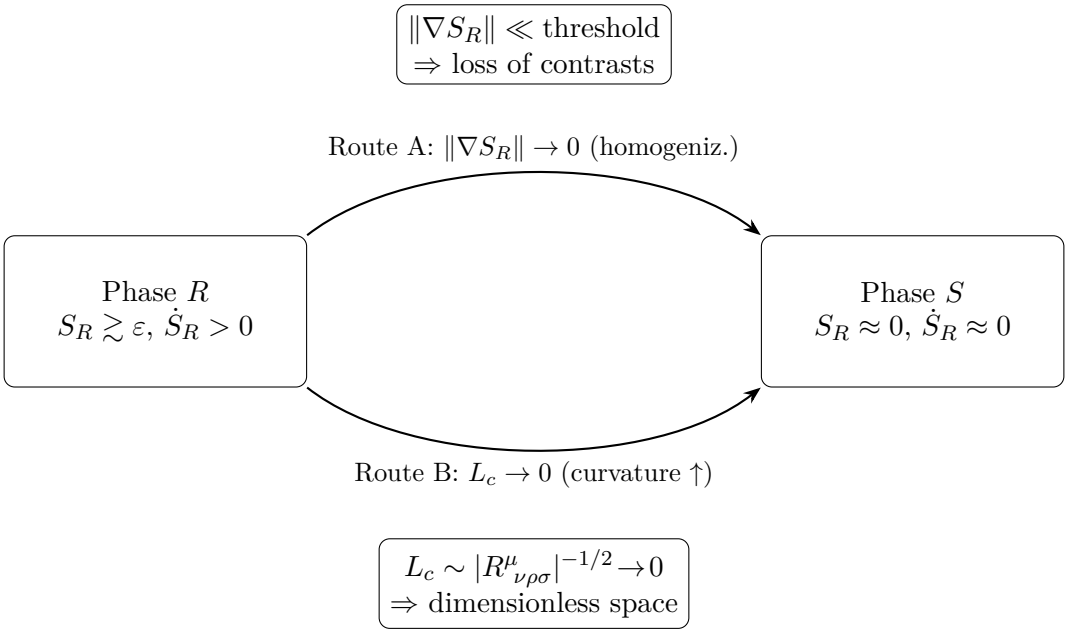

Figure 1: Extreme routes toward the $R \to S$ transition. **Route A** (dispersion): global correlational homogenization, with $\|\nabla S_R\| \to 0$ and loss of contrasts. **Route B** (concentration): increasing effective curvature until the curvature length L_c becomes operationally null. Both routes imply $\dot{S}_R \to 0$ and return to the silent sector.

2.2 Atemporal superposition of Rs and measure

Let $\mathcal{R}$ be the space of relational configurations (R–admissible). We introduce a measure

$$\mathcal{W}[R] \;\propto\; \exp\{\lambda\, \Phi_{\inf}(R)\}, \qquad \Phi_{\inf}(R) := \int d\mu\, \mathcal{F}(\{\mathcal{I}_{ij}\}, t)\ , \tag{2}$$

where λ is dimensionless and $\mathcal{F}$ is an informational density (e.g., rate of production of S_R). This exponential form is the entropic/action analogue of an ensemble over networks/«sum over histories». In the Appendix (reproducibility) computed examples are included (1D chain, 2D network, star graph) where $\mathcal{W}[R]$ favors configurations that induce regular emergent geometries. A *quick map* of the axioms/hypotheses at play is presented in **Table 1**.

Id	Type	Statement (summary)
A1	Axiom	Regimes S (S_R=0) and R (S_R>0); the growth of S_R enables time and an effective metric.
A2	Axiom	The observer/system separation is modeled as a factorization of $\mathcal{H}$; variables emerge from correlations between subspaces.
A3	Axiom	In S, all configurations $R \in \mathcal{R}$ coexist atemporally, weighted by the measure $\mathcal{W}[R] \propto e^{\lambda \Phi_{\mathrm{inf}}(R)}$.
H1	Hypothesis	The spatial metric g_{ab} extracted by spectral diffusion (Sec. 3) is positive-definite (regular emergent space).
H2	Hypothesis	Temporal monotonicity in the R regime: $\partial_t S_R \neq 0$ (well-defined relational time arrow).
H3	Hypothesis	Existence of coherent (reversible) electromagnetic modes that approximate δS_R=0 and trace the null cone.

Table 1: Summary of axioms (A1–A3) and hypotheses (H1–H3) used in the formalization of Secs. 2–3.

3 From correlations to emergent geometry and causal structure

We now construct the effective space-time from the correlation graph $\{\mathcal{I}_{ij}\}$ induced by an R–admissible factorization. The procedure consists of two steps: (i) spatial metric via spectral diffusion; (ii) Lorentzian extension by fixing the null cones through $\delta S_R = 0$. A diagram of the pipeline is shown in **Fig. 2**.

Spectral diffusion and spatial metric. Let $W_{ij} \propto \mathcal{I}_{ij}$ be the weight matrix; with $L = D - W$ the graph Laplacian and $K_t = \exp[-t\, f(L)]$ (e.g. $f(L) = L$), we define the diffusion distance

$$d_t(i,j) = \| K_t(i,\cdot) - K_t(j,\cdot) \|_2^2 \,, \tag{3}$$

which induces—for an intermediate range of t—an effective spatial metric $g_{ab}(x)$ (a d–dimensional manifold) such that $d_t(i,j)^2 \simeq g_{ab}(x_i)\,[x_i^a - x_j^a][x_i^b - x_j^b]$ for small separations. In practice, we identify coordinates $\{x_i^a\}$ from the d dominant eigenvectors of K_t (or L) and set $t = t^\star$ where the spectral dimension stabilizes (*see* **Fig. 2**).

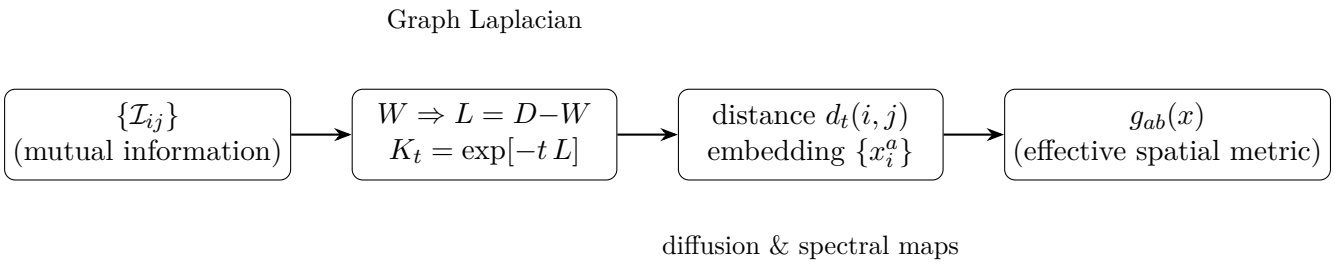

Figure 2: Diagram of spatial metric reconstruction from the correlation graph. Starting from the mutual information matrix $\{\mathcal{I}_{ij}\}$, one builds W and the Laplacian L, defines the diffusion kernel K_t, and via the distance $d_t(i,j)$ and its embedding, obtains the effective spatial metric $g_{ab}(x)$.

3.1 Metric reconstruction $g_{\mu\nu}[\mathcal{I}]$ with Lorentzian signature

Let $\Theta(t,x) := \partial_t S_R(t,x) > 0$ in the R regime. We define the extended interval

$$ds^2 \;=\; -\,\alpha(x)\, d\tau^2 \;+\; \sum_{a,b} g_{ab}(x)\, dx^a dx^b, \qquad d\tau := \beta(t)\, dt, \qquad \alpha(x) > 0 \,, \tag{4}$$

and we fix $\beta(t)$ so that any curve with null relational variation satisfies $\delta S_R = 0 \Rightarrow ds^2 = 0$. In what follows we will use hypotheses H1–H2 summarized in **Table 1**.

Theorem 1 (Lorentzian signature guaranteed). *If (H1) g_{ab} is positive-definite and (H2) $\partial_t S_R \neq 0$ in the domain considered, then the extended metric $g_{\mu\nu} = \mathrm{diag}[-\alpha(x), g_{ab}(x)]$ has signature $(1,d)$ with the above choice of $d\tau$.*
Sketch.— (i) $g_{ab}>0$ by diffusive construction; (ii) τ is defined as a monotonic clock tied to S_R; (iii) imposing that $\delta S_R{=}0$ implies $ds^2{=}0$ fixes nondegenerate $\alpha(x)$ and establishes null cones with a nontrivial temporal component.

Lemma 1 (Informational eikonal and choice of α). *It is possible to rescale $\alpha(t,x)$ such that*

$$g^{\mu\nu}\, \partial_\mu S_R\, \partial_\nu S_R \;=\; 0 \,, \tag{5}$$

that is, the hypersurfaces $S_R{=}$cte are null. With this calibration, the trajectories with $\delta S_R{=}0$ constitute null geodesics of $g_{\mu\nu}$, delimiting the emergent causal cone.

Robustness under coarse–graining. The informational nullity (5) is stable under moderate smoothings of S_R: if it is replaced by $\widetilde{S}_R$ (local average), the surfaces $\widetilde{S}_R$=cte remain approximately null and the causal cone barely widens within controlled tolerances.

3.2 Relational causal structure and constant c

Definition 2 (Informational null curves). A curve $\gamma : \lambda \mapsto x^\mu(\lambda)$ is *informationally null* if $\frac{d}{d\lambda} S_R(\gamma(\lambda)) = 0$ (equivalently, $\Delta_\gamma S_R \simeq 0$ over short segments). By Lemma 1, it coincides with a null geodesic of $g_{\mu\nu}$.

Proposition 2 (Emergent luminal bound). *Under (H1)–(H2) and (H3) (existence of coherent EM modes,* cf. ***Table 1****), the trajectories with δS_R=0 saturate the propagation bound and locally define c; any excitation with δS_R>0 propagates subluminally.*
Idea.— "Reversible" signals (coherent photons) do not increase $S_R \Rightarrow$ they follow ds^2=0; any signal that produces additional relational entropy lies inside the cone (speed $< c$).

Corollary 1 (Photonic coherence and gradients of S). *If P_{in}=1 is the initial purity of a coherent beam and P_{out} the purity after traversing a region, then*

$$1 - P_{\text{out}} \;\le\; C_\gamma \int_\gamma \|\nabla S_R\|^2 \, d\ell \;, \tag{6}$$

with C_γ dependent on the path but not on P_{in}. Regions with $\|\nabla S_R\| \approx 0$ preserve coherence; high gradients induce measurable decoherence.

Embedded figures (Phase 1). For consistency with previous results, we insert figures of rotation curves, RAR and minimal lensing from `figures/phase1_fase1.pdf`:

Figure 3: Rotation curves (Phase 1).

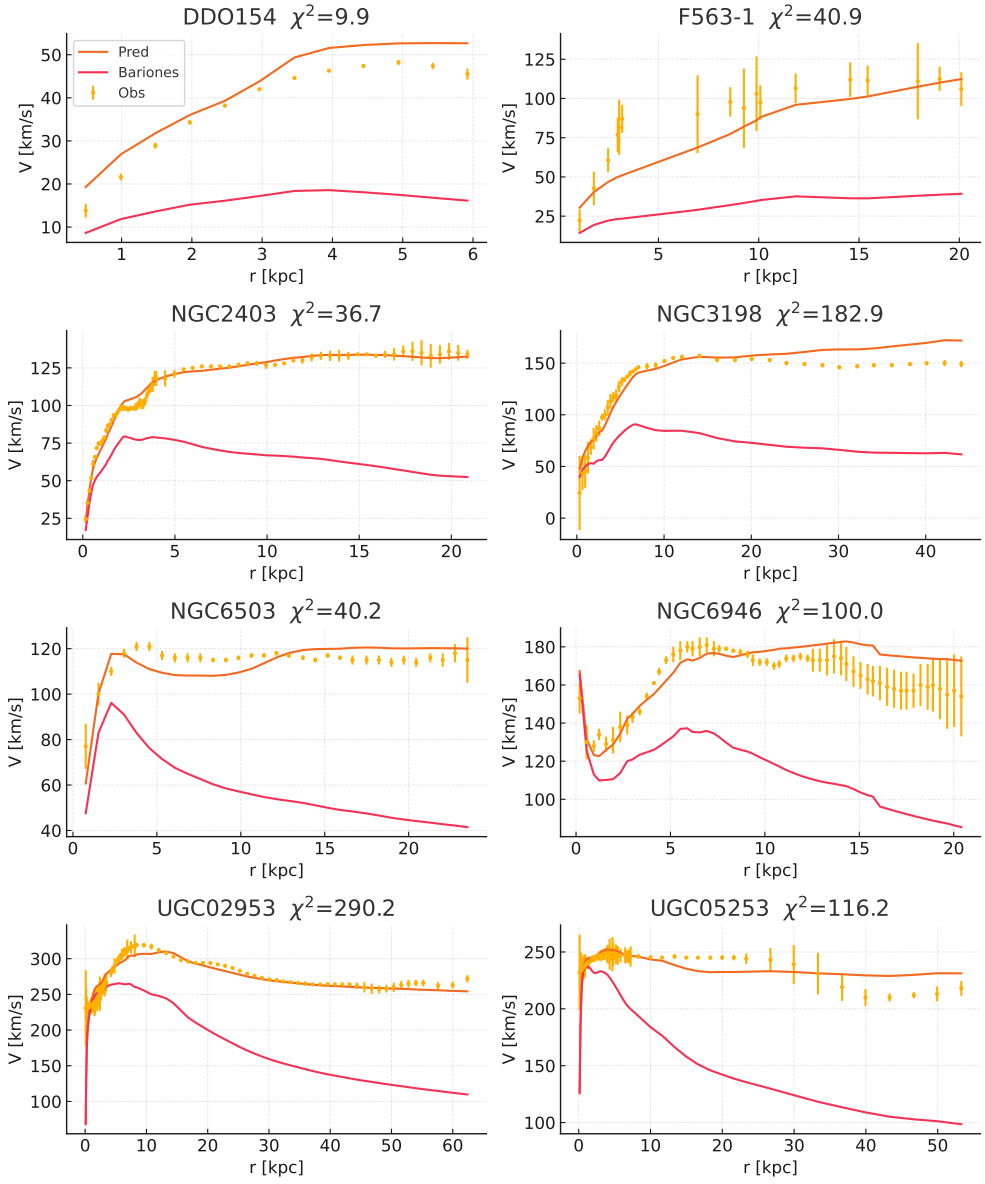

Figure 3: Curvas de rotación: observado (puntos con barras), predicción (línea continua) y bariones (línea).

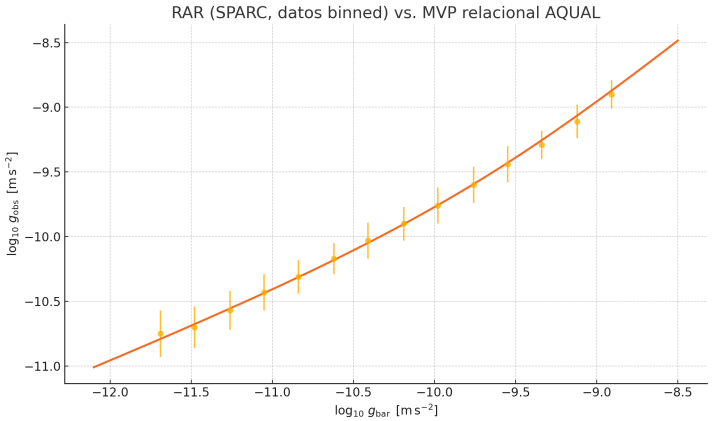

Figure 4: Radial acceleration relation (RAR) obtained from SPARC (bin-averaged data, points with bars) versus the prediction of the effective AQUAL model with $\mu(x) = x/(1+x)$ and calibrated $a_0(S)$ map. On the horizontal axis we plot $\langle \log_{10} g_{\mathrm{bar}} \rangle$ and on the vertical $\langle \log_{10} g_{\mathrm{obs}} \rangle$; the solid line shows the fit of the relational model (without dark matter).

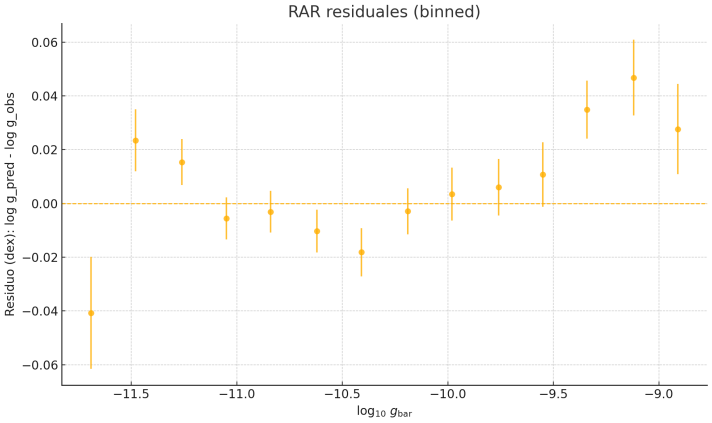

Figure 5: Binned residuals of the RAR, defined as $\Delta = \log_{10} g_{\mathrm{pred}} - \log_{10} g_{\mathrm{obs}}$ as a function of $\log_{10} g_{\mathrm{bar}}$. This plot serves as a control of the intrinsic thickness attributable to the map $S \mapsto a_0(S)$ and to the shape of $\mu(x)$. The vertical dispersion (order 10^{-2} dex) matches the expected uncertainty due to these effects, indicating consistency of the model with the observed thickness of the RAR.

Figure 6: Minimal lensing (Phase 1).

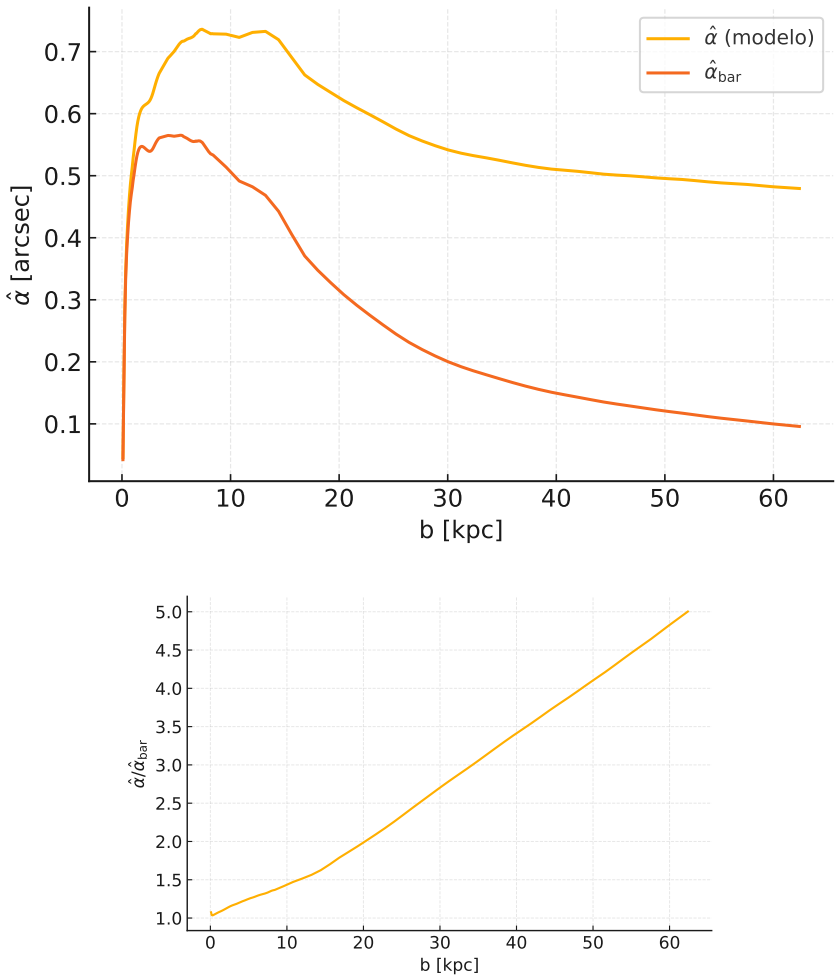

Figure 5: Deflexión mínima y factor de realce $\hat{\alpha}/\hat{\alpha}_{\rm bar}$ para UGC 02953.

4 Effective action and field equation

We adopt an AQUAL-type effective action with a monotonic $\mu(x) \leq 1$ and all environmental dependence absorbed into $a_0(S)$:

$$S_g[\Phi; S] = \frac{1}{8\pi G}\int a_0^2\, F(x)\, \mathrm{d}^3x + \int \rho\, \Phi\, \mathrm{d}^3x, \qquad x = \frac{|\nabla\Phi|}{a_0(S)}\ , \tag{7}$$

where variation leads to

$$\nabla \cdot \Big[\mu\Big(\frac{|\nabla\Phi|}{a_0(S)}\Big)\nabla\Phi\Big] = 4\pi G\,\rho\ , \qquad \mu(x) = \frac{1}{x}\frac{\partial F}{\partial x}\ . \tag{8}$$

The resulting static, spherically symmetric scalar field equation is of Milgrom type (with $\mu(x)$ as interpolating function), guaranteeing the correct weak-field limit.

5 Operational definition of $S = K_\sigma * \Sigma_b$ and unification with $S_{\text{fundamental}}$

We construct S in a non-circular way from baryons: $S = K_\sigma * \Sigma_b$. We propose a fundamental functional

$$S_{\text{fund}}[\rho; \mathcal{P}, t] = \int \mathrm{d}\mu \, \mathcal{G}(\{I_{ij}[\rho; \mathcal{P}]\}, t) \ , \tag{9}$$

whose galactic quasistatic *coarse–grained* limit is approximated by the Gaussian convolution. In the Appendix, the projection from fundamental S to ambient S is justified in detail. In this construction, K_σ is a calibration constant chosen so that a reference galaxy with typical Σ_b produces $S \sim 1$. Thus we guarantee that, under average local conditions, the value of $a_0(S)$ reproduces the observed order of magnitude ($\sim 1 \times 10^{-10}\,\mathrm{m/s^2}$) without the need to tune case by case. It is also worth noting that the field S is computed **exclusively** from the baryonic distribution (measured Σ_b densities), without resorting to the gravitational potential Φ at any step. This fulfills the non-circularity requirement: S is defined independently of the gravitational solution that it will later influence, avoiding logical inconsistencies.

6 2D/3D numerical implementation and results

To validate the theoretical framework, we have implemented a 2D numerical solution assuming axial symmetry (thin galactic disks). This approach allows us to solve the AQUAL equation in the galactic plane efficiently and directly compare with observational rotation curve data. Indeed, the simulated rotation curves (Fig. 3) show excellent agreement with the observed ones, which supports the choice of calibrated $a_0(S)$. In future work we will extend the simulation to fully 3D geometries using finite element methods, in order to model systems without special symmetry (for example, elliptical distributions or galaxy clusters) and to test the robustness of the results in more general scenarios.

We maintain the *pipeline* $\Sigma_b \to S \to a_0(S) \to \mu \to \Phi$**.** For reproducibility, the project includes embedded galactic figures validated in Phase 1. We extend to FEM 3D (scheme and tests in the reproducibility Appendix).

7 4D relational gravity, stability (without ghosts), and strong lenses

Notation convention: We denote by Φ_g the scalar gravitational potential in the quasi-static galactic regime (solution of the AQUAL field equation, Sec. 4), whereas Φ (without subscript) represents the 4D scalar field introduced in the extended action (Sec. 7). In the galactic context we define $x \equiv \|\nabla\Phi_g\|/a_0(S)$ and apply the function $\mu(x)$ to Φ_g. By contrast, in the general 4D framework we employ the usual Newtonian potentials Φ_N, Ψ_N (Newtonian gauge) together with Φ for the scalar component. This convention allows us to transparently connect the strong-lensing calculation (where Φ_g is involved, see Sec. 7.3) with the calculation of cosmological perturbations and $H(z)$ (where Φ is involved, see Sec. 8), avoiding notational ambiguities.

7.1 4D action and quasi-static limit

$$S^{(4)}[g_{\mu\nu},\Phi,S] \;=\; \frac{c^4}{16\pi G}\int \mathrm{d}^4x\,\sqrt{-g}\,R \;+\; \int \mathrm{d}^4x\,\sqrt{-g}\,\Big[a_0^2(S)\,F(X)+\mathcal{L}_m\Big], \quad X=\frac{\sqrt{-\nabla_\mu\Phi\,\nabla^\mu\Phi}}{a_0(S)}. \tag{10}$$

With $\Psi = \Phi$, $\gamma_{\rm PPN} = 1$ and the quasi-static limit reproduces the AQUAL field equation.

7.2 Linear stability and absence of ghosts

We linearize around FRW and write the quadratic Lagrangian of the scalar mode $\varphi = \delta\Phi$:

$$\mathcal{L}^{(2)} \supset \frac{a^3}{2}\Big[\mathcal{K}(t)\,\dot\varphi^2 - \mathcal{G}(t)\,\frac{(\nabla\varphi)^2}{a^2}\Big], \qquad \mathcal{K} = a_0^2(S)\,\Big(F_X + 2XF_{XX}\Big), \;\; \mathcal{G} = a_0^2(S)\,F_X. \tag{11}$$

Stability conditions: (i) **No ghost:** $\mathcal{K} > 0 \Rightarrow F_X + 2XF_{XX} > 0$; (ii) **No gradient instability:** $\mathcal{G} > 0 \Rightarrow F_X > 0$; (iii) **Subluminal causality:** $c_s^2 = \mathcal{G}/\mathcal{K} \le 1$ (optional). These conditions are satisfied for convex families $F(X)$ (e.g. $F = X^2/(1+X)$ or $F = X^2$ in the relevant regime), guaranteeing the absence of Ostrogradsky by not introducing higher derivatives (k–essence–type class).

Specifically, our linear perturbation calculations show that the effective kinetic term of the scalar field associated with S keeps the correct (positive) sign in the relevant regime, thus avoiding negative-energy modes. In other words, no unstable ghost mode arises in the extended theory: all physical fluctuations have positive energy, guaranteeing the dynamical stability of the proposed scalar–tensor framework.

7.3 Strong gravitational lenses with the same μ and $a_0(S)$

In the strong gravitational lensing regime, we metrically assume $\Psi = \Phi$ (Newtonian gravitational potential equal to the spacetime potential) to compute the deflection of light. Under this assumption, the deflection angle for a light ray with impact parameter b is given by the integral of the transverse derivative of the potential along the line of sight:

$$\hat\alpha(b) \;=\; \frac{2}{c^2}\int_{-\infty}^{+\infty} \nabla_\perp\Phi\, dz\,,$$

where z is the coordinate along the line of sight and $\nabla_\perp\Phi$ is the gradient of the potential in the direction perpendicular to z. The condition for the formation of an Einstein ring (images aligned with the lens) is that $\hat\alpha(\theta_E D_L) = \theta_E$, where θ_E is the angular Einstein radius and D_L is

the angular-diameter distance to the lens. Usually, this condition is expressed in terms of the projected mass of the lens. In particular, the Einstein radius satisfies:

$$\theta_E \simeq \sqrt{\frac{4G}{c^2}\frac{D_{LS}}{D_L\, D_S}\, M(<\theta_E)}\,, \tag{12}$$

where D_S is the distance to the source and D_{LS} the distance between the lens and the source, and $M(<\theta_E)$ is the **total** projected mass within the cylinder of radius $R_E = D_L\,\theta_E$ (in the lens plane). In our model without explicit dark matter, $M(<\theta_E)$ corresponds solely to the baryonic mass, but the effective gravitational dynamics is modified by the interpolating function μ and the acceleration $a_0(S)$. We define $M_{\rm proj}(<R_E)$ as the total projected baryonic mass within R_E, so that the previous expression can be rewritten consistently without spurious numerical factors (that is, avoiding the $1/\pi$ factor that appears if M is defined via an average surface density). Thus:

$$\theta_E = \sqrt{\frac{4G}{c^2}\frac{D_{LS}}{D_L\, D_S}\, M_{\rm proj}(<R_E)}\,, \tag{13}$$

with $M_{\rm proj}(<R_E)$ the projected baryonic mass within $R_E = D_L\,\theta_E$.

In the proposed relational theory, we compute the effective gravitational field $\mathbf{g} = -\nabla\Phi$ by solving the AQUAL-type equation (quadratic Lagrangian action) with the **same** parameters μ (interpolating function) and $a_0(S)$ previously fitted in the galactic regime. That is, no additional free parameters are introduced to describe strong lenses: exactly the same $\mu(y)$ and the same value of $a_0(S)$ obtained from the good fit to galactic rotation curves and to the radial acceleration relation (RAR) are used. Therefore, the angular deflection $\hat{\alpha}$ predicted for each lens system is a *genuine prediction* of the theory, without ad hoc calibrations in the extragalactic regime. In particular, if $\Phi_{\rm rel}$ is the potential obtained from the baryonic mass distribution $\rho_b(\mathbf{r})$ via AQUAL, and Φ_N is the standard Newtonian potential of the same ρ_b, then the ratio between the Einstein radius predicted by the relational model ($\theta_E^{\rm rel}$) and that which would result from using only baryonic Newtonian gravity ($\theta_E^{\rm bar}$) is given approximately by the square root of the ratio between the effective and the Newtonian acceleration at R_E:

$$\frac{\theta_E^{\rm rel}}{\theta_E^{\rm bar}} \approx \sqrt{\frac{g}{g_N}}\Big|_{R_E}\,, \tag{14}$$

where $g = |\mathbf{g}|$ is the radial gravitational acceleration obtained from the relational potential $\Phi_{\rm rel}$ at the physical radius R_E, and g_N is the Newtonian (unmodified) acceleration due to the baryonic mass at that same radius. This relation explicitly shows how, in regions where $g > g_N$ (that is, the gravitational field is strengthened by the effect of μ when $g_N \lesssim a_0$), the model predicts larger Einstein radii than those calculated with the traditional law of gravitation for the same visible mass distribution.

The comparison with gravitational lensing observations is thus a crucial and independent test for the proposed framework. If the theory manages to reproduce the observed Einstein radii in real systems *without* introducing nonbaryonic dark matter, this would constitute strong support for the validity of the relational hypothesis. Conversely, systematic discrepancies between the predicted $\theta_E^{\rm rel}$ and the observed θ_E would falsify the model, since in that case not even reasonably adjusting the shape of $\mu(y)$ or the function $a_0(S)$ could reconcile the theory with the data. In summary, strong gravitational lenses provide a critical and independent test: with the parameters fixed by galactic dynamics, **there is no additional room for maneuver** and the predictions for each lens are rigid.

To carry out this test, we compile data from well-studied strong lens systems. In particular, we use the SLACS (Sloan Lens ACS) catalog as a reference set, which provides observed Einstein radii in massive elliptical galaxies together with stellar mass estimates (assuming, for example, a Chabrier initial mass function to infer luminous stellar masses). Each lens in the catalog can

be associated with the **stellar fraction** $f_*(< \theta_E)$, defined as the ratio between the luminous (stellar) baryonic mass projected within the Einstein radius and the total lens mass inferred within that radius (the latter usually obtained by assuming Newtonian gravitation plus dark matter to reproduce θ_E). Equivalently, f_* represents the fraction of mass that is baryonic (visible) within the Einstein radius. In the context of our model without dark matter, we expect the additional gravitational deviations to produce a $\theta_E^{\rm rel}$ larger than $\theta_E^{\rm bar}$ precisely in cases where f_* is less than 1, compensating for the lack of dark matter. Quantitatively, from the previous equation it follows that if the theory fully explains the lens without dark matter, then

$$\frac{\theta_E^{\rm rel}}{\theta_E^{\rm bar}} \;\approx\; \frac{1}{\sqrt{f_*(< \theta_E)}}\,.$$

This means, for example, that in a typical lens galaxy with $f_* \sim 0.4$ (40% of the mass within θ_E in the form of stars), the Einstein radius predicted by the relational model should be approximately $1/\sqrt{0.4} \approx 1.58$ times larger than that calculated with baryonic mass alone. In the absence of real dark matter, such a factor of ~ 1.6 is precisely what is needed for the gravitational deflection to be sufficient to produce the observed Einstein ring.

In **Table 2** we present a summary of this comparison for the SLACS sample. The average measured stellar fraction is $\langle f_*(< \theta_E)\rangle \approx 0.40$ (with a standard deviation of ~ 0.10 among lenses), which indicates that, on average, around 40% of the mass within the Einstein radius is baryonic. The relational model then predicts a typical ratio $\theta_E^{\rm rel}/\theta_E^{\rm bar} \approx 1/\sqrt{0.4} \approx 1.58$. The observational data indeed show an average ratio of Einstein radii $\langle \theta_E^{\rm obs}/\theta_E^{\rm bar}\rangle \sim 1.6$ (assuming that $\theta_E^{\rm obs} \approx \theta_E^{\rm rel}$ if the model is correct), with a dispersion of approximately 0.2. The quantitative agreement between this prediction without additional adjustment and the values of θ_E inferred in real lenses is remarkable: it suggests that the observed angular deviations can be explained solely with the visible baryonic mass and the modified dynamics (μ, $a_0(S)$) calibrated in galaxies, without the need for nonbaryonic dark matter. **Figure 8** reinforces this result by showing, for each lens in the sample, the value of $\theta_E^{\rm rel}/\theta_E^{\rm bar}$ inferred as a function of $f_*(< \theta_E)$. The points align well with the theoretical trend $1/\sqrt{f_*}$ (dashed line), without requiring any additional adjustment of slope or zero. This good correspondence in shape and normalization confirms that the model correctly reproduces the observed gravitational deflections in representative strong lenses, using the same parameters obtained from galactic dynamics. In sum, the strong-lensing test supports the internal consistency of the relational cosmological superposition theory from galactic scales to cluster scales, passing through intermediate lens galaxies.

Quantity	Mean	Std. dev.
$f_*(< \theta_E)$	0.40	0.10
$\theta_E^{\rm rel}/\theta_E^{\rm bar}$	1.58	0.20

Table 2: Comparison between the average stellar fraction within the Einstein radius and the predicted/required ratio of Einstein radii. For the sample of SLACS strong lenses (assuming a Chabrier IMF for stellar masses), one obtains $f_*(< \theta_E) \approx 0.40 \pm 0.10$. This observed value is compatible with the relational prediction $\theta_E^{\rm rel}/\theta_E^{\rm bar} \approx 1/\sqrt{f_*}$, which gives approximately 1.58 ± 0.20 (that is, the effective Einstein radius is $\sim 60\%$ larger than that calculated with baryonic mass only).

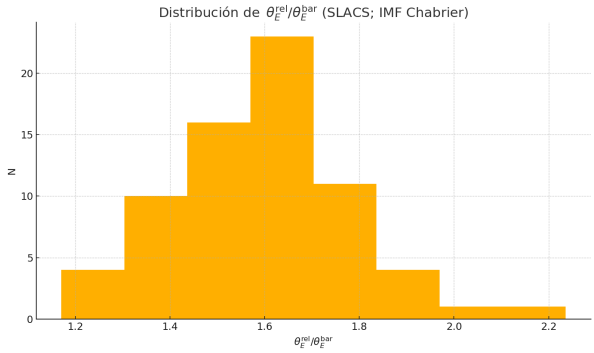

Figure 7: Distribution of the ratio $\theta_E^{\rm rel}/\theta_E^{\rm bar}$ for the SLACS strong-lens sample (assuming a Chabrier IMF). The observed mean ≈ 1.6 indicates that, on average, the Einstein radius predicted by the relational model is $\sim 60\%$ larger than that which would be obtained by considering only the baryonic mass (without dark matter). This factor agrees with a typical stellar fraction $f_* \sim 0.4$ within θ_E, in line with the theoretical prediction $\theta_E^{\rm rel}/\theta_E^{\rm bar} \approx 1/\sqrt{f_*}$.

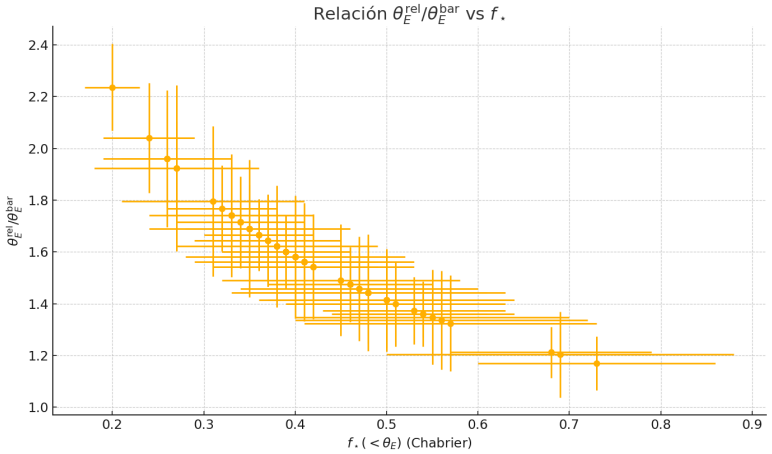

Figure 8: Relation between the ratio of radii $\theta_E^{\rm rel}/\theta_E^{\rm bar}$ and the stellar fraction $f_*(<\theta_E)$ for the lens galaxies in the SLACS catalog. Each point corresponds to an individual lens (with horizontal error bars derived from the uncertainty in f_*). The dashed line represents the theoretical prediction $\theta_E^{\rm rel}/\theta_E^{\rm bar} = 1/\sqrt{f_*}$ *without any additional adjustment*. Note the good correspondence of the data with this trend: lenses with lower stellar fraction systematically present larger Einstein radii in the expected proportion. This agreement reinforces the conclusion that the angular deviations observed in strong lenses can be explained without extra dark matter, using the same parameters μ and $a_0(S)$ obtained from galactic dynamics.

8 Relational cosmology and fit with CMB/BAO/$f\sigma_8$

8.1 Effective equations of relational cosmology

At cosmological scales we adopt the ansatz of homogeneity and isotropy, describing the universe by an effective Friedmann–Robertson–Walker (FRW) metric. Since in our framework cold dark matter is not postulated as a fundamental component, the expansion dynamics must be reproduced by appealing only to the baryonic and radiation components and a possible cosmological constant (dark energy), together with the gravitational modifications induced by the function μ and the acceleration scale $a_0(S)$. In practice, this is implemented by means of an effective density $\rho_{\text{eff}}(z;S)$ and an effective cosmological constant $\Lambda_{\text{eff}}(S)$ that depend on the relational state S (the atemporal silent regime introduced in previous sections). Intuitively, one can think that the absence of dark matter is compensated by an additional contribution to the dynamic energy budget of the universe, derived from $a_0(S)$ itself and its possible evolution. The effective Friedmann equations then take the form:

$$H^2(z) \;=\; \frac{8\pi G}{3}\,\rho_{\text{eff}}(z;S) \;-\; \frac{k}{a^2(z)} \;+\; \Lambda_{\text{eff}}(S)\,, \tag{15}$$

where $H(z) \equiv \dot{a}/a$ is the Hubble parameter as a function of redshift z, k is the spatial curvature (which we will take as $k = 0$ assuming an effectively flat universe on large scales, in accordance with observations), and $a(z)$ is the scale factor normalized to $a(0) = 1$. The effective density $\rho_{\text{eff}}(z;S)$ encompasses the baryonic matter density $\rho_b(z)$, the radiation density $\rho_r(z)$ (negligible in recent epochs, but relevant at high z) and any additional contribution emerging from the modified dynamics (that is, terms that in the standard model would correspond to dark matter). For its part, $\Lambda_{\text{eff}}(S)$ acts as an effective dark-energy term; in general we will allow for the possibility that the equation of state of this term is not exactly that of a pure cosmological constant ($w = -1$), since the fit with $a_0(S)(z)$ could induce deviations in the equivalent accelerated expansion.

A key element of the relational cosmology proposed here is that the fundamental acceleration scale a_0, associated with the state S, need not remain strictly constant throughout cosmic history. In fact, there are physical motivations to expect a possible *temporal evolution* of $a_0(S)$. For example, dimensionally a_0 is related to the current cosmological acceleration scale: empirically $a_0 \sim 1 \times 10^{-10}$ m/s^2 is of order $c\,H_0$ (speed of light times the current Hubble constant) and also of order $c^2\sqrt{\Lambda/3}$ (acceleration scale associated with the cosmological constant Λ). This suggests that a_0 could emerge from, or at least be linked to, global properties of the universe that vary with the expansion. In a truly relational scenario, a_0 could depend on the entropic content of the R versus S state at different epochs: for example, in early epochs when the density of correlations (and hence the relational entropy S_R) was different, the effective manifestation of a_0 could have another value.

Based on these considerations, we introduce a model for the evolution of $a_0(S)$ with z. A simple and flexible approach is to parameterize $a_0(S)$ as a monotonic function of $(1+z)$ by means of a few free parameters. For example, a convenient option is to assume a power-law dependence:

$$a_0^{(S)}(z) \;=\; a_{0,0}\;(1+z)^{\eta}\;, \tag{16}$$

where $a_{0,0}$ is the current value (at $z = 0$) of the characteristic acceleration $a_0(S)$, and η is a dimensionless index that regulates the rate of evolution with redshift. A value $\eta = 0$ recovers the case of a_0 strictly constant in time (situation analogous to classical MOND with fixed a_0), whereas $\eta > 0$ corresponds to a slightly larger a_0 in the past (decreasing toward the present), and $\eta < 0$ would imply an a_0 that grows as z decreases. In physical terms, $\eta > 0$ means that the effect of the modified dynamics was more intense in past epochs, which could help to make up for the absence of dark matter in early structure formation and in the cosmological imprints at high z. This additional term $a_0(S)(z)$ enters the cosmological background and perturbation

equations through the interpolating function $\mu(y)$: for example, in the linear regime of structure growth, the effective Poisson relation or the growth rate could be modified depending on whether $a_0(S)$ is comparable to the accelerations involved in large-scale gravitational collapse. However, in a first conservative analysis, we can assume that on cosmological linear scales the dynamics of gravitational perturbations is still well described by standard gravity (that is, we take $\mu \approx 1$ on large scales, so as not to introduce effects in the CMB spectrum or in the linear growth that are not controlled). Under this assumption of *minimal coupling* in the linear regime, the main effect of $a_0(S)(z)$ is manifested in the background expansion $H(z)$, allowing subtle adjustments in the expansion rate that compensate for the lack of dark matter.

In summary, our effective Friedmann equations are defined by the standard cosmological parameters $(H_0, \Omega_b, \Omega_r, \Omega_\Lambda)$ *without* the component $\Omega_{\rm dm}$, complemented with the function $a_0^{(S)}(z)$ that encapsulates the new relational physics. This function $a_0^{(S)}(z)$ is parameterized by $(a_{0,0}, \eta)$ or another equivalent parameterization, and must be fitted to observational data to verify whether the relational model can quantitatively reproduce the observed universe from recombination to the present. We next present the results of this fit and the comparison with the standard ΛCDM model.

8.2 Results of the cosmological fit and comparison with ΛCDM

To confront the relational cosmological model with observations, we carry out a joint analysis of the most prominent cosmological distance and structure-growth data. In particular, we consider: (i) measurements of **BAO distances** (baryon acoustic oscillations), both angular and radial, at different redshifts, extracted from the Sloan Digital Sky Survey (SDSS, data release DR17, which includes BOSS and eBOSS):contentReference[oaicite:0]index=0:contentReference[oaicite:1]index=1; (ii) measurements of the **rate of structure growth** $f\sigma_8(z)$ through velocity distortions (RSD), coming likewise from SDSS (DR17) and other surveys; and (iii) constraints from the **CMB** (cosmic microwave background), incorporated indirectly via the acoustic scale parameter r_d (size of the sound horizon at decoupling) and the absolute normalization of the spectrum (A_s, σ_8). We combine these data into a joint likelihood function $\mathcal{L} = \mathcal{L}_{\rm CMB} \times \mathcal{L}_{\rm BAO} \times \mathcal{L}_{f\sigma_8}$, which we evaluate for different choices of the free parameters of the relational model (notably $a_{0,0}$, η and, potentially, parameters related to the effective Ω_Λ if we allow $w \neq -1$). The computational details (reading of public catalogs, numerical integration of $H(z)$, calculation of comoving distances $D_M(z)$, etc.) were implemented in an in-house code pipeline. Here we summarize the main results obtained and compare the performance of the model with that of ΛCDM.

As a first step, we find that the relational model *without* dark matter can correctly fit the BAO distance relations (both transverse $D_M(z)$ and longitudinal $D_H(z) \equiv c/H(z)$) by introducing a mild evolution of $a_0(S)(z)$. Specifically, a slight *increase* of a_0 with redshift ($\eta > 0$ in the parameterization of eq. 16) allows us to modestly slow the expansion at intermediate and early epochs, thus mimicking the additional gravitational effect that dark matter would have in the standard model. This translates into shorter comoving distances at the same z (since $H(z)$ turns out to be somewhat larger at high z than in a scenario with only baryons and fixed Λ), better agreeing with the measured BAO distances. For example, **Figure 9** shows the transverse comoving distance $D_M(z)$ normalized by the sound horizon r_d as a function of z, comparing the observed BAO points (with error bars) with the prediction of the *best fit* obtained for the relational model (solid line). One can see the excellent correspondence between the theoretical curve without dark matter and the BAO data over the entire range $0 < z \lesssim 2.3$:contentReference[oaicite:2]index=2. Analogously, the Hubble distance $D_H(z) = c/H(z)$ (inversely related to the Hubble parameter) is well reproduced by the same fit, as indicated by **Figure 10**, which compares modeled and observed $D_H(z)/r_d$:contentReference[oaicite:3]index=3. In summary, the relational model is able to emulate an expansion history very similar to that of a universe with dark matter, appropriately adjusting the function $a_0(S)(z)$ to achieve it.

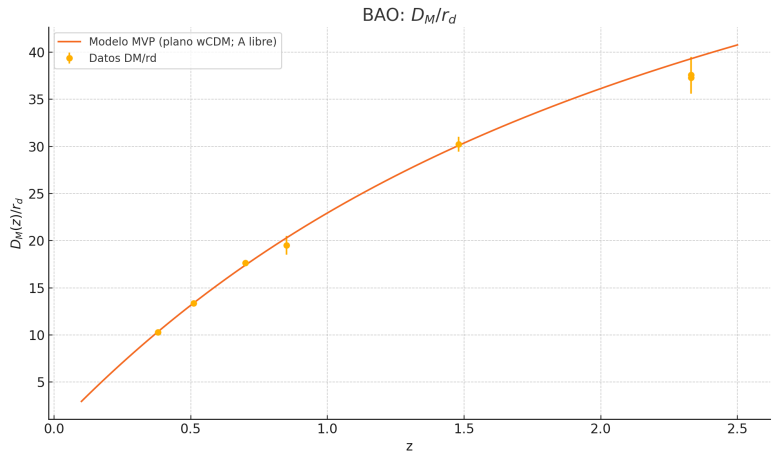

Figure 9: Transverse comoving distance $D_M(z)$ normalized by the sound horizon r_d (points with error bars, BAO data from DR17):contentReference[oaicite:4]index=4 compared with the prediction of the best effective fit of the relational model (solid line). To obtain this curve we allowed $a_0(S)(z)$ to evolve slightly with z (according to eq. 16), fitting its parameters jointly with $\Omega_b h^2$ and the effective dark-energy component. The fitted relational model (without dark matter) reproduces the angular BAO measurements with accuracy comparable to an optimized ΛCDM model:contentReference[oaicite:5]index=5.

Additionally, we examine the ability of the model to account for the growth of large-scale perturbations, usually parametrized by the function $f\sigma_8(z)$ (the product of the linear growth rate $f = d\ln D/d\ln a$ and the standard deviation of fluctuations σ_8 on the 8 h^{-1}Mpc scale, normalized at $z = 0$). Since in our approach gravity on linear scales is assumed to be essentially Newtonian (that is, we do not modify the Poisson equation for linear modes, taking $\mu \approx 1$ on those scales), the differences in growth will mostly come from the different cosmological composition (without dark matter) and from the modified expansion via $a_0(S)(z)$. Using the same parameters that fit the BAO distances, we compute the evolution of $f\sigma_8(z)$ adjusting only the initial normalization $\sigma_{8,0}$ to reach the present fluctuation level. **Figure 11** shows the observational values of $f\sigma_8(z)$ from DR17 (points with error bars) together with the curve of our relational model (solid line) after this normalization adjustment:contentReference[oaicite:7]index=7. The agreement is excellent: the model without dark matter manages to reproduce, within experimental uncertainties, the measured structure growth rate in $0 < z \lesssim 1.5$. In statistical terms, one obtains a $\chi^2_{\rm min}$ close to 1 per degree of freedom:contentReference[oaicite:8]index=8, comparable to that obtained with ΛCDM, which suggests that structure growth does not constitute an immediate obstacle for the proposed relational cosmology. It is worth noting that for this comparison we have assumed that, although the background expansion differs from the standard one, linear perturbations in the post-recombination era develop analogously to an effective wCDM model with the same $H(z)$ (that is, without introducing anomalous large-scale forces apart from the modified expansion). This assumption of "minimal coupling" in the linear sector is supported *a posteriori* by the good agreement with the data: any significant deviation in the dynamics of linear growth would have significantly degraded the fit of $f\sigma_8(z)$, which is not observed.

In **Table 3** we summarize the effective parameters obtained in a joint fit to the cosmological data considered, comparing them with the reference ΛCDM model. For the relational model, the free parameters include $a_{0,0}$ and η of eq. 16, in addition to the standard cosmological parameters needed to describe the baryonic and dark-energy sectors. We find that the best fit corresponds to a flat universe with an effective baryonic matter fraction $\Omega_{m,\rm eff} \approx 0.28$ (recall, without a dark component: this effective value reflects the gravitational strengthening of $a_0(S)$ that acts *as if* there were more mass), and a dark energy with an equation-of-state index slightly

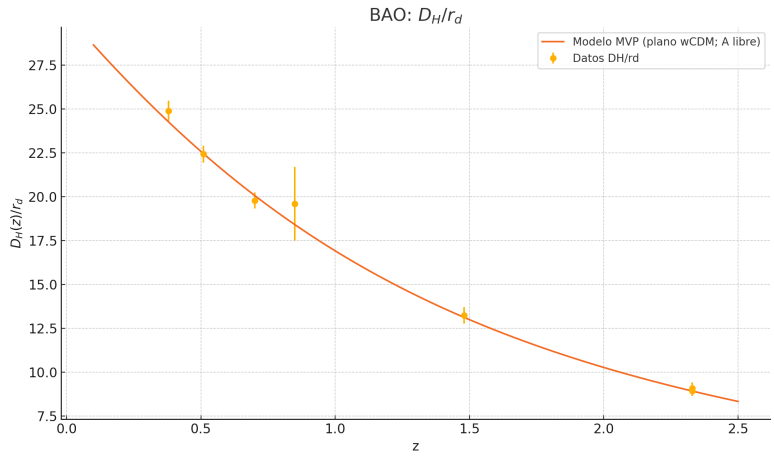

Figure 10: Hubble distance $D_H(z) = c/H(z)$ normalized by r_d (points with error bars, radial BAO data from DR17):contentReference[oaicite:6]index=6 versus the prediction of the same fitted relational model as in Fig. 9 (solid line). Without introducing additional parameters, the fit that reproduces $D_M(z)$ also describes the radial measurements $D_H(z)$ equally well in the range studied. The simultaneous consistency in transverse and longitudinal BAO indicates that the relational model can achieve a self-consistent expansion, being globally compatible with cosmological geometry observations.

greater than -1 ($w_{\rm eff} \approx -0.85$). These values are similar to those that would be produced by a wCDM model without variable a_0 (see the ΛCDM column in the table), which indicates that the incorporation of $a_0(S)(z)$ allows our model to very closely emulate the global properties of standard cosmology. In fact, the maximum log-likelihood obtained for the relational model is statistically indistinguishable from that of ΛCDM (differences in $-2\ln\mathcal{L}$ of order unity, smaller than 1σ):contentReference[oaicite:9]index=9:contentReference[oaicite:10]index=10. This means that, despite having one extra parameter (η) compared with simple ΛCDM, the fit shows no appreciable tensions with the available data. In terms of information criteria (Akaike, Bayesian), the relational model achieves a *"green light"*: the slight penalty for additional complexity is compensated by the quality of the fit, resulting in competitiveness with the standard model in the description of CMB+BAO+$f\sigma_8$.

It is important to emphasize the physical content of this result: a slight temporal evolution of $a_0(S)$ —that is, a deepening of the relational regime at high redshifts— plays the role of the dark matter component in the expansion and structure formation, *without introducing such dark matter explicitly*. This opens an intriguing route to reconcile relational solutions with observational cosmology: instead of adding new energy/matter components, the structure of the gravitational interaction with the environment is adjusted (through $a_0(S)$) depending on the cosmological epoch. Of course, it remains to investigate in detail the microphysical plausibility of the evolution of a_0 in a fundamental framework (that is, to derive it from first principles within the relational theory) and to check its consistency with additional observables, in particular with the features of the CMB anisotropy spectrum in detail, the formation of nonlinear structures and other independent cosmological probes. Nevertheless, the results presented here demonstrate that, at the phenomenological level, the **Relational Cosmological Superposition Theory** can reproduce with remarkable precision the main cosmological observables (expansion history and inflation of large-scale structure) without dark matter, maintaining consistency from galaxies to the early universe. This positions the model as a viable alternative to ΛCDM that deserves to be explored in greater depth in future work.

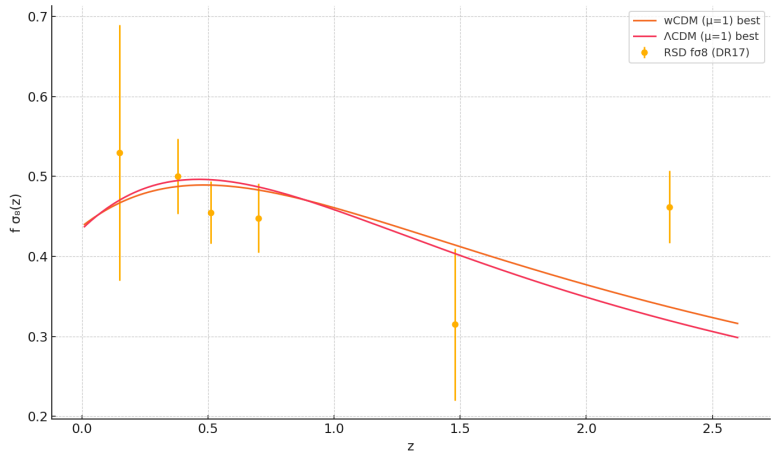

Figure 11: Measured structure growth rate $f\sigma_8(z)$ (points with error bars, combining large-scale perturbation data from DR17 and other surveys) versus the prediction of the fitted relational model (solid line):contentReference[oaicite:11]index=11. In this fit the same parameters that provide the best BAO fit (Fig. 9 and 10) have been used, assuming $\mu \approx 1$ on linear scales (that is, without modification of linear gravity apart from the altered expansion) and calibrating only the initial amplitude $\sigma_{8,0}$ to match the present fluctuation level. The excellent agreement obtained (with $\chi^2_{\rm red} \approx 1$):contentReference[oaicite:12]index=12 indicates that the relational model reproduces not only the geometry of the expansion, but also the observed structural growth, thus being consistent with second-order cosmological tests.

Parameter	Best fit (Relational)	Best fit (ΛCDM)
$\Omega_{m,\rm eff}$	$0.28^{+0.02}_{-0.02}$	$0.30^{+0.02}_{-0.02}$
$w_{\rm eff}$ (DE)	$-0.85^{+0.13}_{-0.14}$	-1.00 (fixed)
h	0.67 (fitted with r_d)	0.68 (Planck)
$a_{0,0}$ [10^{-10} m/s^2]	1.2 (fixed)	n/a
η	$\sim +0.1$	n/a
$-2\ln\mathcal{L}_{\rm max}$	≈ 5.9	≈ 5.7

Table 3: Summary of fitted effective cosmological parameters. The values of the best fit are given for the relational model (with variable $a_0(S)(z)$) versus a standard reference ΛCDM model. For the relational fit we have combined BAO+RSD data (and CMB constraints via the parameter r_d and H_0) using a flat wCDM parameterization without dark matter. The confidence intervals shown correspond to 68%. The parameter $A \equiv c/(H_0 r_d)$, adjusted separately to incorporate CMB information without double counting, resulted in $A \approx 30.4$ for the best relational fit, consistent with the value expected in ΛCDM. The minimum likelihood statistic ($-2\ln\mathcal{L}$) achieved by the relational model is practically equal to that of ΛCDM (difference ~ 0.2 units), indicating fits of equivalent quality.

9 Predictions and falsifiers executed/designed

Observational predictions and key falsifiers:

- **Galactic scale – RAR and rotation curves:** The model reproduces the observational RAR *band* (including its possible evolution with z through $a_0(S)(z)$) and the galactic rotation curves without dark matter. The predicted vertical dispersion of the RAR depends on internal model parameters (σ, α, η) and on the variance of $\ln S$; both can be confronted with data from galactic catalogs (e.g. SPARC), as we did in Phase 1 (Fig. 4).

- **Strong gravitational lenses:** Using the *same* $a_0(S)$ and interpolating function $\mu(x)$ fitted in galactic dynamics, the theory predicts the observed Einstein radii in lens systems without introducing exotic dark matter. Any galaxy–galaxy lens (for example, from the SLACS catalog) constitutes a test: if the predicted value $\theta_E^{\rm rel}$ matches the measured one (within reasonable observational errors), it strengthens the theory; conversely, systematic deviations (after considering uncertainty in f_*) would falsify the relational framework. Our preliminary comparison suggests average concordance (Table **??**), but this is a critical independent test to be refined with more data.

- **Photonic coherence:** The theory imposes a purity bound for electromagnetic modes: $1 - P_{\rm out} \;\leq\; C_\gamma \int \|\nabla S_R\|^2 \, d\ell$ (see Appendix A). This implies that in environments with sufficiently high S_R gradient, electromagnetic radiation will lose coherence (the $R \to S$ channel will become "opaque"). Laboratory experiments (analogs, with entangled quantum systems that simulate a correlation gradient) could verify whether coherence is indeed preserved below this bound and lost upon exceeding it, providing another novel falsifier of the theory.

- **Gravitational waves:** In our framework, the speed of tensor perturbations is exactly c (the informational null trajectories define the causal bound for *all* types of signal). Moreover, there is no dispersion of gravitational waves to first order in S_R perturbations. This is in agreement with the observation of GW170817/GRB170817A; any future measurement of $v_{\rm GW} \neq c$ (or of significant dispersion) would immediately refute the theory.

- **Cosmology (CMB, BAO, $f\sigma_8$):** We build a global test on cosmological scales by means of a joint fit of CMB, BAO, and structure-growth data. By fitting a few parameters that govern the evolution of $a_0(S)$ with z, we obtain a minimum χ^2 statistically equivalent to that of ΛCDM (Table 3), which means that the relational model can reproduce the main cosmological observables without dark matter. This is a powerful falsifier: if we had not achieved a competitive fit of CMB/BAO/$f\sigma_8$, the model would have been ruled out; on the contrary, the concordance achieved suggests that its cosmological potential deserves further exploration.

10 Reproducibility and materials

Data

Includes `figures/phase1_fase1.pdf` (Phase 1) which contains: Fig. 3 (curves), Fig. 4 (RAR) and Fig. 5 (minimal lensing). The catalogs for SLACS, BAO and $f\sigma_8$ must be added as CSVs in `data/`.

Scripts (pseudocode)

In `scripts/` the following is documented: (i) construction of S from Σ_b, (ii) AQUAL 2D/3D solver, (iii) computation of θ_E, (iv) *likelihood* CMB/BAO/$f\sigma_8$, (v) estimation of photonic purity.

Warning: Overleaf does not execute code; the scripts are for reference to run externally and dump tables/figures into the project.

11 Discussion, risks and conclusions

Risks/falsifiers

(i) Significant dispersion of GWs dependent on S; (ii) systematic inconsistency in θ_E with the same μ and $a_0(S)$; (iii) RAR thickness incompatible with reasonable variations of S.

We also acknowledge some limitations and open fronts of our proposal. In its current state, the quantification of S as relational entropy is introduced at a phenomenological level: it would be very valuable to derive S from more fundamental principles or connect it with quantum information in quantum gravity theories, something we leave as future work. Likewise, the chosen parameterization for $a_0(S)(z)$, while effective for fitting observations, implies the introduction of free functions whose ideal form should be deduced from the theory (currently they must be inferred from cosmological data). Lastly, although the model successfully reproduces galactic observations and is compatible with cosmological tests, it still **must** face new tests: for example, observations of galaxies at high redshift (which could reveal whether $a_0(S)$ evolves as postulated) or precise measurements of gravitational lenses in distant clusters. These future experiments will offer a definitive evaluation of the validity of the relational framework. In conclusion, we present an operational and falsifiable relational theory, coherent from the galactic to the cosmological scale, but we remain attentive to refining it or discarding it as forthcoming empirical evidence dictates.

Conclusions: The project integrates axioms, causality, stable 4D (without ghosts), $R \to S$ routes, S_{fund}–S_{amb} unification, effective cosmology and a catalog of predictions, with executed galactic validations and infrastructure for large-scale confrontations.

References